Unusual Aggressive Breast Cancer: Metastatic Malignant Phyllodes Tumor

Adam Singer[1*], Jonathan Tresley[1], Jose Velazquez-Vega[2], Monica Yepes[3]

1. Department of Radiology, Jackson Memorial Hospital, Miami, Florida, USA

2. Department of Pathology, Jackson Memorial Hospital, Miami, Florida, USA

3. Department of Radiology, Sylvester Comprehensive Cancer Center, University of Miami Miller School of Medicine, Miami, Florida, USA

* **Correspondence:** Adam D. Singer, M.D., Jackson Memorial Hospital, Department of Diagnostic Radiology, West Wing 279, 1611 NW 12th Avenue, Miami, FL 33136, USA
(*AdamSinger82@gmail.com*)

Radiology Case. 2013 Feb; 7(2):24-37 :: DOI: 10.3941/jrcr.v7i2.1430

ABSTRACT

For the year of 2012, it has been estimated that breast cancer will account for the greatest number of newly diagnosed cancers and the second highest proportion of cancer related deaths among women. Breast cancer, while often lumped together as one disease, represents a diverse group of malignancies with different imaging findings, histological appearances and behavior. While most invasive primary breast cancers are epithelial derived adenocarcinomas, rare neoplasms such as the phyllodes tumor may arise from mesenchymal tissue. Compared to the breast adenocarcinoma, the phyllodes tumor tends to affect a younger population, follows a different clinical course, is associated with different imaging and histological findings and is managed distinctively. There may be difficulty in differentiating the phyllodes tumor from a large fibroadenoma, but the mammographer plays a key role in reviewing the clinical and imaging data in order to arrive at the correct diagnosis. Early diagnosis with proper surgical management can often cure non-metastatic phyllodes tumors. However, in rare cases where metastasis occurs, prognosis tends to be poor. This report describes the presentation, imaging findings and management of a metastatic malignant phyllodes tumor.

CASE REPORT

INTRODUCTION

For the year of 2012, it has been estimated that breast cancer will account for the greatest number of newly diagnosed cancers and the second highest proportion of cancer related deaths among women [1]. Breast cancer, while often lumped together as one disease, represents a diverse group of malignancies with different imaging findings, histological appearances and behavior. Most invasive primary breast cancers are epithelial derived adenocarcinomas with the most common histological subtype being the invasive ductal adenocarcinoma accounting for approximately 75% of cases [2]. Overwhelmingly diagnosed in women and arising from mesenchymal tissue, phyllodes tumors (PTs) are rare breast cancers which account for between 0.3 and 1% of primary breast cancers [3,4] (Table 1). Unfortunately, there are similarities between the primary breast adenocarcinoma and the PT which can make differentiation difficult. The PT also shares much in common with the benign fibroadenoma. Therefore, in order to ensure prompt and correct treatment, it is imperative that the mammographer uses all of the available information to make the correct diagnosis.

The clinical presentation of the PT is different compared to that of the breast adenocarcinoma. First, while both the breast adenocarcinoma and PT can occur at any age, the mean age of diagnosis of breast cancer in general in women is 61 [11]. In contrast, multiple studies have shown that the diagnosis of the PT tends to occur at an earlier age [4,5,8,9,10]. In a review of seventeen studies each describing at least twenty patients or more diagnosed with PTs, Parker et al. determined that the mean age at diagnosis is 45, twenty years older than the typical age range of fibroadenoma proliferation [12]. By contrast, the peak age range of fibroadenoma detection has been described as 20-25 years old [19]. Second, the PT tends to be larger than the adenocarcinoma and is classically characterized by rapid growth. Parker et al. describe cases of tumors becoming as large as forty centimeters (cm) in diameter. While these clinical findings help in making the diagnosis of a PT, they are not specific. The next step in working up such a breast lesion involves imaging. Unfortunately, although there are imaging findings that aid in making the diagnosis of a PT, none are pathognomonic. Unlike other commonly encountered breast lesions, percutaneous biopsy is often not sufficient to arrive at a conclusive diagnosis because there are histopathological similarities between the fibroadenoma and the PT. Moreover, percutaneous biopsy may result in insufficient sampling because the behavior of the tumor is determined by the most malignant cells. Therefore, excisional biopsy is often required to make a definitive diagnosis [19]. The excisional biopsy is also the treatment of choice because even the benign PT is well known for local aggressiveness.

In this manuscript, a patient diagnosed with metastatic malignant PT is described and the multimodality imaging findings of the metastases are characterized. The aims include adding information to the relatively small database of PT imaging findings and to describe imaging findings typical of the PT, the histopathological correlation and current management strategies.

CASE REPORT

A 43 year old Latin female from Honduras with no significant past medical history presented with a palpable left breast mass which she first noticed five months prior to admission. She noted that over the two months leading up to her admission, this mass had rapidly increased in size and was associated with pain and pruritus. The patient experienced menarche at the age of 12, gave birth to five children starting at the age of 22, did not breast feed and denied prior use of oral contraceptives or hormonal replacement therapy. She had no history of prior chest radiation therapy and had no known family history of PT. Upon initial physical examination, the patient was afebrile with normal vital signs. Examination of the left breast revealed a very large lobulated mass with thinning of the overlying skin, nipple inversion and no palpable axillary or supraclavicular lymphadenopathy. The right breast was normal. The patient could not tolerate mammography due to the size of the tumor. A contrast enhanced computed tomographic (CT) study of the chest, abdomen and pelvis was performed to evaluate the breast mass and for the presence of metastatic disease. A large, heterogeneous left breast mass that measured 19 x 24 x 25 cm was visualized. The mass was mostly cystic (measuring -9.1 Hounsfield units), but contained thick, irregular enhancing septations and was surrounded by a thick enhancing wall (Figure 1). The mass abutted the left pectoralis major muscle. Also identified were bilateral pulmonary nodules, the largest of which measured 6 mm.

A percutaneous biopsy of the breast mass was performed which revealed a high grade malignant spindle cell neoplasm representing either a metaplastic sarcomatoid carcinoma or a malignant PT (not shown). Given the bulk of the tumor and the patient's resultant discomfort, mastectomy was elected. During surgery, the mass was noted to invade the pectoralis major muscle necessitating partial resection. A left pectoralis major flap was utilized for reconstruction. Following resection, the mass weighed 16 pounds. Pathologically, the mass was described as a high grade PT with sarcomatous overgrowth (Figure 2). Immunohistochemistry was positive for CD10 and negative for ER, PR, HER2, CD34, desmin, S100, p63 and CK903. The negative CK903 and p63 excluded the possibility of a myoepithelial or squamous spindle cell carcinoma and the negative S100 and CD34 excluded the possibility of a myofibroblastic or neurogenic sarcoma.

One month following the surgery, the patient became aware of a soft tissue mass growing at the mastectomy scar. Upon physical examination, there were post surgical changes consistent with a left mastectomy and a new parasternal 10 cm non-mobile, non-tender mass fixed to the medial portion of the scar. There was no palpable axillary lymphadenopathy. A non-enhanced CT of the chest was performed which demonstrated a lobulated soft tissue mass superficial to the sternum that measured 9 x 6 x 8 cm without definite involvement of the sternum, although periosteal reaction was identified. (Figure 3A and C). Bilateral stable pulmonary nodules were again visualized. The patient was started on Adriamycin and ifosfamide. Following two cycles, a contrast enhanced CT of the chest demonstrated that the mass had a cystic component, with a thick, irregular, enhancing wall and enhancing septations and now measured 13 x 7 x 9 cm (Figure 3B). Stable pulmonary nodules and sternal periosteal reaction was identified. Due to progression in spite of therapy, the decision was made to treat with radiation therapy and gemcitabine. After completing chemotherapy and radiation with a total dose of 5000 cGy, the patient underwent resection of the parasternal mass. The mass was removed en bloc with partial resection of the sternum, the bilateral third, fourth and fifth ribs and the bilateral costal cartilages of ribs six and seven. Upon exposure of the lungs, multiple bilateral lung masses were visualized four of which were biopsied. A rectus abdominis free flap was used to reconstruct the anterior chest wall. Histopathologically, the chest wall mass contained pleomorphic tumor cells and areas of treatment related necrosis (Figure 4).

Two months later, the patient noted diminished ability to use her right lower extremity due to worsening right hip pain. A femoral radiograph was obtained and a permeative pattern with associated periosteal reaction was visualized in the

proximal femur (Figure 5). These findings were concerning for metastatic disease and a Technetium 99m (Tc99m) labeled methylene diphosphonic acid (MDP) bone scan confirmed new radiotracer uptake in the proximal femur corresponding to the radiographic abnormality, not present on a bone scan obtained eight months previously (Figure 6). Subsequently, a CT guided bone biopsy was performed (Figure 7) which confirmed the presence of a spindle cell tumor consistent with the patient's known history of malignant PT. Next, magnetic resonance imaging (MRI) of the femur was acquired (Figure 8) to evaluate disease extent and to aid in surgical planning which showed a soft tissue mass adherent to the femur with diffuse infiltration of the cortical and medullary bone. The mass measured 4.0 x 4.4 x 2.1 cm and demonstrated low T1 signal intensity, contrast enhancement and high T2 signal intensity. The increased T2 signal intensity and enhancement both within the soft tissue surrounding the mass and within the vastus lateralis muscle raised suspicion for local invasion. The underlying femoral cortex was thinned and in some places was destroyed. The marrow signal intensity in the involved portion of the proximal femur was markedly abnormal with low T1 signal intensity, high T2 signal intensity and heterogenous areas of enhancement, mostly peripherally. Upon surgical excision, invasion of the vastus lateralis muscle was confirmed necessitating partial resection. The proximal right femur was resected and a megaprosthesis was placed. The gross specimen demonstrated tumor adherent to the femur with diffuse tumor infiltration of the medullary cavity (Figure 9), compatible with the MRI findings. Light microscopy again verified the presence of spindle cell tumor cells confirming the diagnosis of metastatic PT (Figure 10).

One month later, the patient presented to the emergency department with shortness of breath. A CT demonstrated significant progression of disease (Figure 11) with a large necrotic left breast mass invading the chest wall. Additionally, there was a large necrotic right axillary mass that measured 11 x 10 x 9 cm. Also identified were a right breast mass and multiple large pleural based masses, the largest of which measured 13 x 5 cm. There were numerous pulmonary nodules, some of which were new, areas of pulmonary parenchymal consolidation and a left pleural effusion. At this point, the decision was made to transition towards palliative care and the patient was discharged to home hospice.

DISCUSSION

With the first reported case in 1838 by Johannes Müller, PTs derive their name from their histological appearance that is characterized by a leaf like architecture containing varying degrees of epithelial and mesenchymal elements. The epithelial component tends to line thin cystic spaces, hence the historical (but no longer used) name cystosarcoma phyllodes. The mesenchymal cells represent the neoplastic portion of the PT. The epithelial component is essential for making the diagnosis of a phyllodes tumor because in its absence, the presence of spindle shaped cells suggests an alternative diagnosis such as a sarcoma [12].

After a patient presents with a breast mass that is clinically concerning for a PT, imaging studies must be performed. Although non-specific, the imaging findings may aid in making the correct and timely diagnosis (table 2). The first step in management should be a mammogram. Mammographically, the PT usually appears as a hyperdense, large, rounded or lobulated mass with distinct margins [8,10,13,19]. In a study of 51 patients with PTs, 96% were non-spiculated masses. In this same study, larger tumor size was shown to correlate with a higher likelihood of malignancy. A size greater than 3 cm had a relative risk of malignancy of 3.87 ($p < 0.004$) while all tumors larger than 8 cm were malignant. Microcalcifications within a PT are unusual, especially those calcifications more commonly associated with ductal carcinoma in situ or invasive ductal carcinoma such as fine linear branching calcifications. If calcifications are present, they tend to be coarse [8]. Tan et al. speculate that the tendency of PTs to lack microcalcifications is due to the rapid tumor growth. Liberman et al. was able to estimate doubling time in five cases of phyllodes tumors and found that the doubling time for a single case of a malignant PT was 36 days, while the median doubling time of the four benign PTs was 211 days [13]. In another study of 34 PTs, the calculated median growth rate for the combined borderline and malignant tumors was 105% per month and 17% per month for benign tumors [19]. Gordon et al. analyzed a group of 194 breast lesions diagnosed as fibroadenomas by fine needle aspiration that were subsequently followed over time and found that an increase in size of up to 20% over a six month interval was consistent with a lesion that was benign [14]. These authors also stated that a mass with a size greater than 3 cm should be considered for excision because of an increased risk of representing a PT [14]. Percutaneous biopsy, while useful in evaluating epithelial derived neoplasia, may be less accurate when attempting to differentiate a fibroadenoma from a PT. In a group of 17 patients with PTs, Foxcroft et al. were able to make the correct diagnosis utilizing percutaneous core biopsy in 65% of cases. Fine needle aspiration (FNA) fared worse. Among 57 cases of PTs evaluated with FNA, the diagnosis was suggested in 13 cases (22.8%). In this group evaluated by FNA, 22 were diagnosed as fibroadenomas (38.5%). It is also important to note that the pathophysiology of PT proliferation is different than that of ductal and lobular cancer. Since the malignant cells are not associated with epithelial elements, the likelihood of ductal type microcalcifications typically regarded as suspicious is low. However, there are reported cases of epithelial derived breast cancer arising within a PT [16,17]. Therefore, the presence of suspicious microcalcifications in a mass that is otherwise concerning for a PT does not exclude the diagnosis of adenocarcinoma and a concomitant ductal carcinoma should be entertained in the differential.

Following mammography, breast ultrasound is the imaging modality of choice to characterize a breast mass and suspected PT. Sonographically, not only is it difficult to differentiate a PT from a fibroadenoma, but the ability to grade a PT with ultrasound is also limited [8]. In a study of the 24 PTs, half were diagnosed by ultrasound preoperatively as fibroadenomas [8]. In this same study, the only characteristic that statistically significantly differentiated between benign and borderline or malignant tumors was an irregular shape (X2

= 5.754, p = 0.039) , which the authors speculated was related to different rates of proliferation within the high grade portions of the tumor. An irregular shape was described in 66.7% of malignant PTs, 90.9% of borderline PTs and 25% of benign PTs. One sonographic characteristic all of these tumors had in common was an overall heterogeneous appearance. In general, most authors describe the PT appearance, regardless of grade, as hypoechoic. Authors have described small cystic clefts which are sometimes visible and have been attributed to the cystic areas visualized pathologically. It has been suggested that their presence may indicate higher grade PTs. Clefts with a mean diameter of 8 mm were described in 4/9 and 3/21 malignant and benign PTs, respectively, but the difference between the two grades lacked statistical significance (p = 0.15) [13]. In another study including 78 PTs with available ultrasound examinations, Foxcroft et al. found cystic clefts or macrocysts associated with 4/5 malignant PTs. However, these clefts were found in 18 non-malignant PTs in the same study [19]. In another case, after utilizing mammography, breast ultrasound, breast MRI and percutaneous biopsy, El Khouli et al. described a case of a 25-year-old with an enlarging breast mass that measured 3 x 3 cm which required excisional biopsy to make the diagnosis of a giant fibroadenoma [18]. More recently, breast imagers have been utilizing ultrasound as a method to determine the relative elasticity of tumors. Adamietz et al. found that in eight cases of PTs, all had a relatively elastic center surrounded by an inelastic periphery, which the authors termed the "ring sign" [15].

MRI also may play a role in the evaluation of a suspected PT. In general, PTs are often described as heterogeneous. In one study of 21 PTs and 81 fibroadenomas, 71% of the PTs had a heterogeneous internal structure while only 41% of the fibroadenomas were described similarly [20]. On T1 weighted (T1W) sequences, the mass is usually either isointense or hypointense. However, hemorrhage has been documented to occur within these tumors which will result in foci of increased T1 signal intensity [8]. T2 weighted (T2W) sequences may be hypointense with the exception of focal areas of hyperintensity when there are cystic spaces or clefts present [20]. Necrosis may also result in increased T2 signal intensity. These masses often have internal septations that are hypointense on both T1 and T2 weighted sequences. Following the administration of intravenous contrast, these tumors often demonstrate rapid enhancement although the septations usually do not enhance. However, in the authors' institution, there was one case of a pathologically proven benign PT with enhancing septations (figure 12). In one study, 33% of the PTs imaged with MR had suspicious enhancement kinetics [20]. Although the sample size is low, Wurdinger et al. finds that focal increased T2 signal around the mass is seen in 21% of PTs, but in only 1.2% of fibroadenomas (p =0.005) [20].

The role of CT is usually to assess for the degree of local invasion, recurrence or for the presence of metastasis. Since the workup of a breast mass typically does not include a CT, large studies evaluating the CT appearance of a PT have not been published. Suzuki-Uematsu et al. described a case of a malignant PT evaluated with contrast enhanced CT where the 10 x 10 cm mass was described as having a peripheral enhancing rim which is concordant with the CT findings of the patient described in this manuscript.

Currently, there are few reports describing the imaging appearance of osseous PT metastases. In this report, we describe such findings across four imaging modalities. While metastasis can present as a solid mass adjacent to the involved bone, it appears to rapidly infiltrate the cortex and medulla resulting in a permeative pattern on radiographs and CT. Bone scan may show increased Tc99m-MDP radiotracer uptake. Correspondingly, MRI may show a diffusely infiltrated bone with complete marrow replacement, avid enhancement, cortical destruction and significant surrounding soft tissue edema. More importantly, if surgical resection is to be considered, the MRI may better delineate the metastasis extent into the surrounding tissues which would aid the surgeon in terms of approach.

The PT is classified on the basis of its histological grade as benign, borderline or malignant. Grading is determined by evaluating the frequency of observed mitoses, the characteristics of the tumor margins, the stromal cellularity and the degree of atypia [5,12]. Another histological finding which is worrisome for increased aggressiveness is stromal overgrowth, defined as the presence of stroma without associated epithelial elements over one low power (x 40) field [13]. It has been estimated that 60% are benign, 20% are borderline and the remaining 20% are malignant [3]. With increasing tumor grade, studies have shown that the risk of metastasis increases [5,12]. In addition to grade, specific pathological findings have been shown to correlate to recurrence and metastasis with statistical significance. Chen et al. found that in patients with positive surgical margins, 6/13(46%), recurred locally, while only 13/159 (8%) with negative margins did (p = 0.00018). In terms of risk for metastasis, the same authors found that stromal cellularity, stromal overgrowth, stromal atypia, mitotic activity, tumor margin status and heterologous stromal elements correlated with statistical significance (p = 0.032, 0.00002, 0.004, 0.005 and 0.046, respectively) [5]. These authors also noted that of the three patients with metastases, all three were initially graded as benign and that all three eventually succumbed to their disease.

Regardless of grade, the primary method of treatment is surgical. Options include local excision, wide local excision and mastectomy. Wide excision is recommended because of the strong tendency for local recurrence (up to 20%), even in benign PTs [20]. In a study of 172 patients with PT conducted by Chen et al., local excision was defined as removal of the mass with no more than a 0.5 cm tumor free margin while wide local excision was defined as removal of the mass with at least a 1.0 cm tumor free margin. Of the 172 patients, 76% were benign, 7% were borderline and 17% were malignant. There was a tendency for less aggressive surgical treatment of lower grade tumors with mastectomy performed in 10% of benign cases, 67% of borderline cases and 86% of malignant cases. Local recurrence occurred only in the benign cases treated with local or wide local excision with a rate of approximately 15% [5]. When metastatic, lymph node involvement is rare with authors noting a rate of approximately 10% [4,5]. Among

42 patients who underwent a modified radical mastectomy, none had lymph node involvement [5]. Similarly, in a study with axillary nodal dissection performed in 42 patients with either PT or primary breast sarcoma, 2 patients had lymph node involvement, one of which was from a malignant PT [4]. In a third review, lymph node involvement was noted in 3/15 cases (20%) [3]. Secondary treatments include adjuvant radiotherapy and/or chemotherapy. These adjuvant therapies are rarely utilized and in one study, two received adjuvant radiation therapy and three received adjuvant chemotherapy [5]. Of the two patients that received radiation therapy, one diagnosed with a malignant PT and the other with a borderline PT, neither had recurrence or metastasis. Of the three who received chemotherapy, two began after detection of metastasis and died within six months time. The third, diagnosed with a borderline PT, remained disease free. In another study, survival of six patients diagnosed with either benign or borderline PTs had a 100% survival rate at 3 years, while of the 13 diagnosed with malignant PTs, 3 years survival was 53.8% [4]. However, in this study, some patients received adjuvant therapy although the specifics regarding which patients are unclear. Suzuki-Uematsu et al. reviewed 15 cases of malignant PTs and described a five year survival rate following primary surgery of 10% while the 2.2 year survival rate following detection of metastasis was 11%.

In conclusion, the phyllodes tumor is a rare mixed mesenchymal and epithelial primary breast neoplasm which affects a younger cohort of patients than the more common primary epithelial derived breast adenocarcinoma. Depending on histopathological characteristics, the tumor behavior may range from benign with a similar surgical response compared to that of the fibroadenoma, to local aggressiveness to distant metastasis with associated poor prognosis. A key to the successful management of this tumor may be early detection and resection prior to the development of distant metastasis. Given the low incidence of this tumor and the current lack of specific clinical and imaging characteristics to make this diagnosis, more pooling of data may be beneficial to identify specific findings that increase pre-test probability prior to making a decision whether to observe the mass or proceed to surgery.

TEACHING POINT

The phyllodes tumor is a rare mesenchymal primary breast cancer that occurs in middle aged women, exhibits rapid growth and shares many clinical, imaging and histopathological similarities with the benign fibroadenoma. At a size between 3-5 cm, consideration for excisional biopsy should be entertained.

REFERENCES

1. Siegel R, Naishadham D, Jemal A. Cancer statistics, 2012. CA Cancer J Clin. 2012 Jan-Feb;62(1):10-29. PMID: 22237781.

2. Li CI, Uribe DJ, Daling JR. Clinical characteristics of different histologic types of breast cancer. Br J Cancer. 2005 Oct 31;93(9):1046-1052. PMID: 16175185.

3. Suzuki-Uematsu S, Shiraishi K, Ito T, Adachi N, Inage Y, Taeda Y, Ueki H, Ohtani H. Malignant phyllodes tumor composed almost exclusively of a fibrosarcomatous component: a case report and review of malignant phyllodes tumors with metastases. Breast Cancer. 2010 Jul;17(3):218-224. PMID: 19350353.

4. Confavreux C, Lurkin A, Mitton N, Blondet R, Saba C, Ranchère D, Sunyach MP, Thiesse P, Biron P, Blay JY, Ray-Coquard I. Sarcomas and malignant phyllodes tumours of the breast--a retrospective study. Eur J Cancer. 2006 Nov;42(16):2715-2721. PMID: 17023158.

5. Chen WH, Cheng SP, Tzen CY, Yang TL, Jeng KS, Liu CL, Liu TP. Surgical treatment of phyllodes tumors of the breast: retrospective review of 172 cases. J SurgOncol. 2005 Sep 1;91(3):185-194. PMID: 16118768.

6. Konstantakos AK, Graham DJ. Cystosarcoma phyllodes tumors in men. Am Surg. 2003 Sep;69(9):808-811. PMID:14509333.

7. Lee JW, Nadelman CM, Hirschowitz SL, Debruhl ND, Bassett LW. Malignant phyllodes tumor of a genotypic male, phenotypic female with liposarcomatous differentiation. Breast J. 2007 May-Jun;13(3):312-313. PMID: 17461912.

8. Tan H, Zhang S, Liu H, Peng W, Li R, Gu Y, Wang X, Mao J, Shen X. Imaging findings in phyllodes tumors of the breast. Eur J Radiol. 2012 Jan;81(1):e62-69. Epub 2011 Feb 25. PMID: 21353414 .

9. Bernardi G, Cavallaro G, Indinnimeo M, Fiore A, Basso L, D'Ermo G, De Toma G, Cavallaro A. Usefulness of ultrasounds in the management of breast phyllodes tumors. G Chir. 2012 Mar;33(3):81-85. PMID: 22525552.

10. Harvey JA. Unusual breast cancers: useful clues to expanding the differential diagnosis. Radiology. 2007 Mar;242(3):683-694. PMID: 17325062.

11. Data on SEER (Surveillance, Epidemiology and End Results) cancer statistics available at http://seer.cancer.gov/csr/1975_2009_pops09/results_single/sect_01_table.11_2pgs.pdf (Accessed on 10/17/12).

12. Parker SJ, Harries SA: Phyllodes tumours. Postgrad Med J 2001;77:428-435. PMID: 11423590.

13. Liberman L, Bonaccio E, Hamele-Bena D, Abramson AF, Cohen MA, Dershaw DD. Benign and malignant phyllodes tumors: mammographic and sonographic findings. Radiology. 1996 Jan;198(1):121-124. PMID: 8539362 .

14. Gordon PB, Gagnon FA, Lanzkowsky L. Solid breast masses diagnosed as fibroadenoma at fine-needle aspiration

biopsy: acceptable rates of growth at long-term follow-up. Radiology. 2003 Oct;229(1):233-238. PMID: 14519878.

15. Adamietz BR, Kahmann L, Fasching PA, Schulz-Wendtland R, Uder M, Beckmann MW, Meier-Meitinger M. Differentiation between phyllodes tumor and fibroadenoma using real-time elastography. Ultraschall Med. 2011 Dec;32 Suppl 2:E75-79. Epub 2011 Dec 22. PMID: 22194044.

16. Nio Y, Iguchi C, Tsuboi K, Maruyama R. Ductal carcinoma in situ arising within a benign phyllodes tumor: A case report with a review of the literature. Oncol Lett. 2011 Mar;2(2):223-228. Epub 2010 Dec 8. PMID: 22866068.

17. Nomura M, Inoue Y, Fujita S, Sakao J, Hirota M, Souda S, Ohshima M. A case of noninvasive ductal carcinoma arising in malignant phyllodes tumor. Breast Cancer. 2006;13(1):89-94. PMID: 16518067.

18. El Khouli RH, Louie A. Case of the season: a giant fibroadenoma in the guise of a phyllodes tumor; characterization role of MRI. Semin Roentgenol. 2009 Apr;44(2):64-66. PMID: 19233082.

19. Foxcroft LM, Evans EB, Porter AJ. Difficulties in the pre-operative diagnosis of phyllodes tumours of the breast: a study of 84 cases. Breast. 2007 Feb;16(1):27-37. Epub 2006 Jul 28. PMID: 16876413.

20. Wurdinger S, Herzog AB, Fischer DR, et al: Differentiation of phyllodes breast tumors from fibroadenomas on MRI. AJR Am J. Roentgenol 185:1317-1321, 2005. PMID: 16247156.

21. Schnitt, SJ. and Collins, LC. (2009). Fibroepithelial Lesions. In Biopsy Interpretation of the Breast. Pages 153-180. Pennsylvania, USA: Lippincott Williams & Wilkins.

22. Tavassoli, F.A., Devilee, P. (Eds): World Health Organization Classification of Tumours. Pathology and Genetics of Tumours of the Breast and Female Genital Organs. IARC Press: Lyon 2003.

23. Tavassoli, F.A. (1992) Biphasic Tumors. In Pathology of the Breast, Second Edition. Pages 598-611. McGraw-Hill.

FIGURES

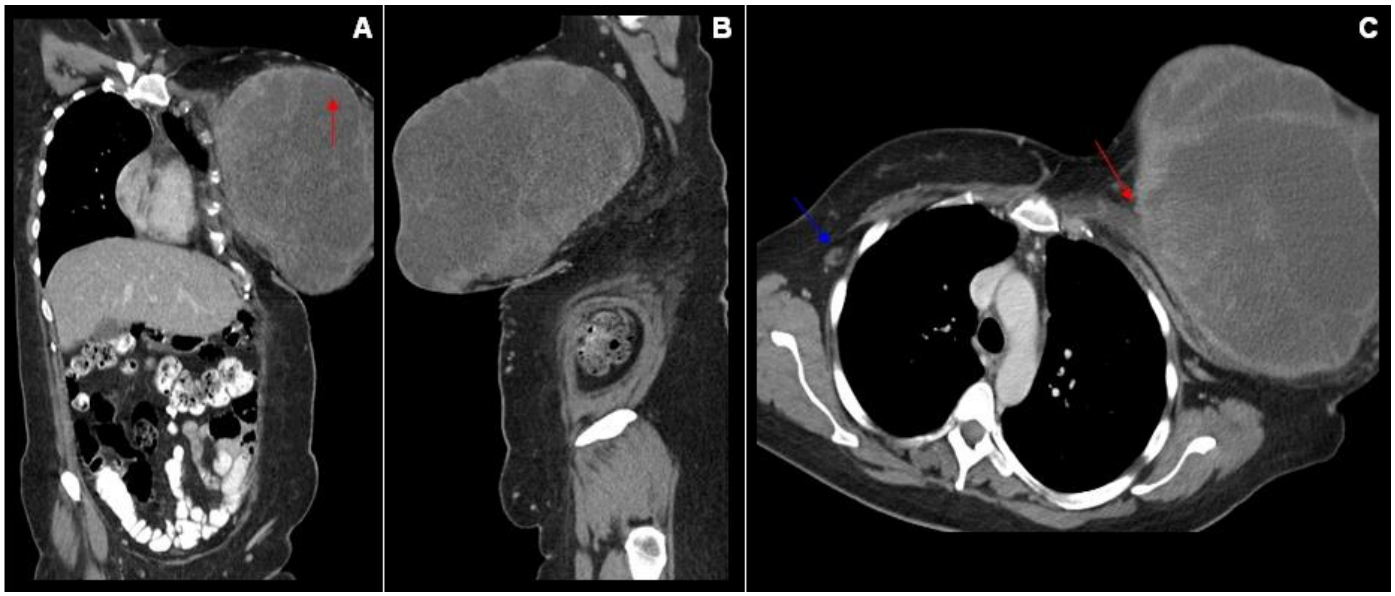

Figure 1: 43 year old female with malignant phyllodes tumor. Contrast enhanced CT of the chest, abdomen and pelvis. 410 mAs, 120 kVP, 1.5 and 5.0 millimeter (mm) slices.
1A: Coronal CT (abdominal window, ww/wl 400/40): Large heterogeneous left breast mass measuring 19 x 24 x 25 cm which is mostly cystic but contains thick enhancing septations and is surrounded by a thick, irregular enhancing wall. The area indicated by the arrow measures -9.1 Hounsfield Units (HU).
1B: Sagittal CT (abdominal window): Large heterogeneous left breast mass as seen in 1A.
1C: Axial CT (abdominal window): Large heterogeneous breast mass which abuts the left pectoralis major muscle. There is no fat plane between the mass and the muscle (red arrow). There is a normal appearing right axillary lymph node (blue arrow). No abnormal lymph nodes were identified.

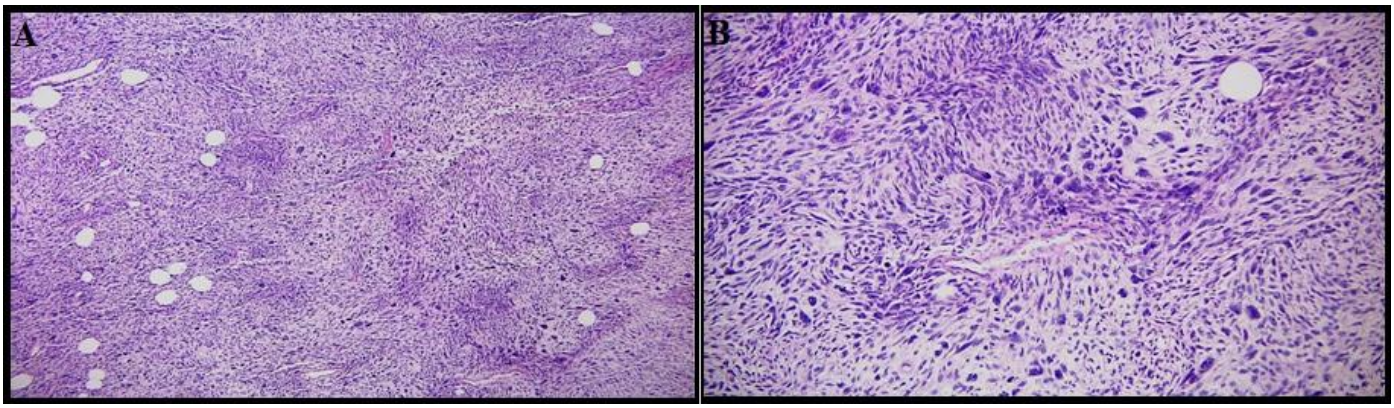

Figure 2: 43 year old female with malignant phyllodes tumor.
2A: Sarcomatous overgrowth in a malignant phyllodes tumor with numerous pleomorphic spindle cells and increased mitotic activity. The absence of epithelial elements in this magnification characterizes the sarcomatous overgrowth in this tumor. Hematoxylin and eosin (H&E) section, 4x magnification.
2B: Numerous malignant pleomorphic cells are evident in this magnification. H&E section, 10x magnification.

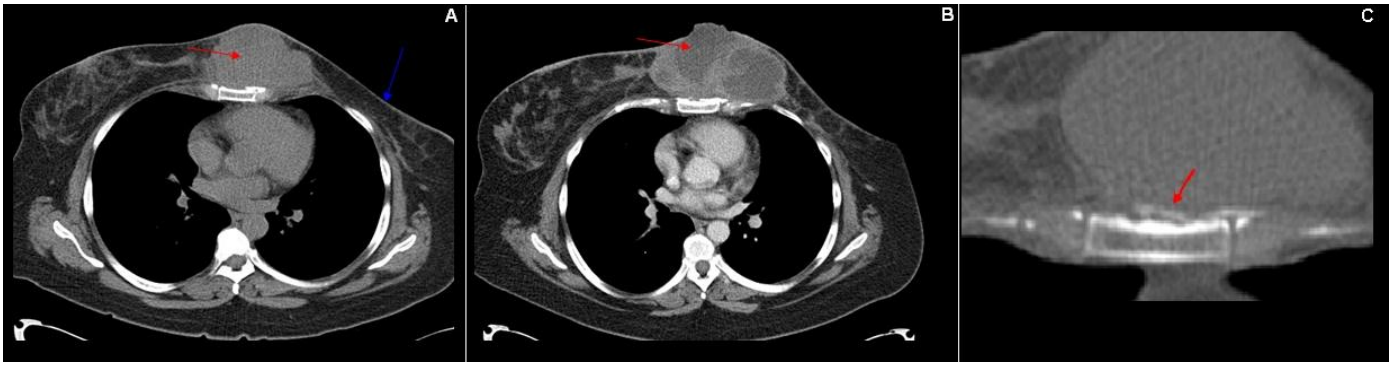

Figure 3: 43 year old female with malignant phyllodes tumor. CT of the chest. 76 mAs, 120 kVP, 5.00 mm slices.
3A: Non-enhanced axial CT of the chest (abdominal window): Large parasternal soft tissue mass (red arrow). There are post-surgical changes consistent with left mastectomy (blue arrow).
3B: Contrast enhanced axial CT of the chest (abdominal window): 3 months after 3A was acquired, the heterogeneous soft tissue mass has increased in size despite chemotherapy. Like the primary breast mass, this mass is mostly cystic (red arrow) with thick enhancing septations and a thick irregular wall.
3C: Non-enhanced axial CT of the chest (bone window, magnified): Large soft tissue mass adjacent to the sternum. Periosteal reaction around the sternum is present (red arrow).

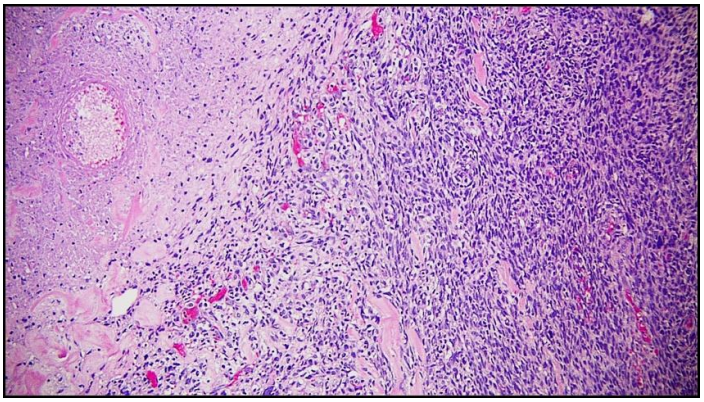

Figure 4 (left): 43 year old female with malignant phyllodes tumor. Chest wall mass showing metastatic malignant phyllodes tumor with an area of necrosis consistent with treatment effect. H&E section, 10x magnification.

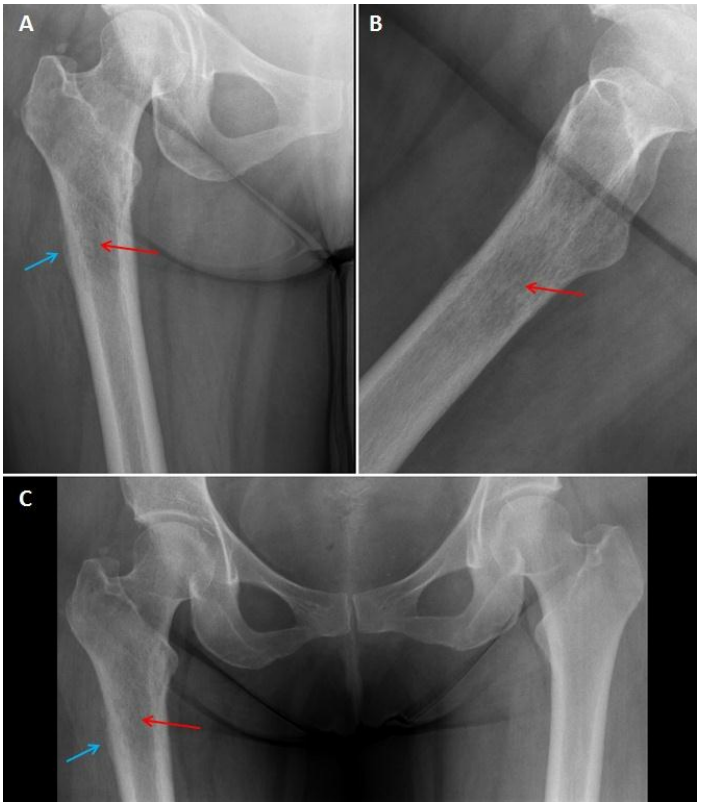

Figure 5 (left): 43 year old female with malignant phyllodes tumor. Femur radiographs.
5A and B: AP and lateral views of the right femur: There is an aggressive appearing lesion with a permeative pattern (red arrow) extending from the greater trochanter inferiorly where there is a wide zone of transition within the medullary cavity.
5C: AP view of the pelvis: There is an aggressive appearing lesion with a permeative pattern (red arrow) extending from the greater trochanter inferiorly where there is a wide zone of transition within the medullary cavity. There is periosteal reaction along the lateral margin of the femoral cortex (blue arrow). The left femur is normal.

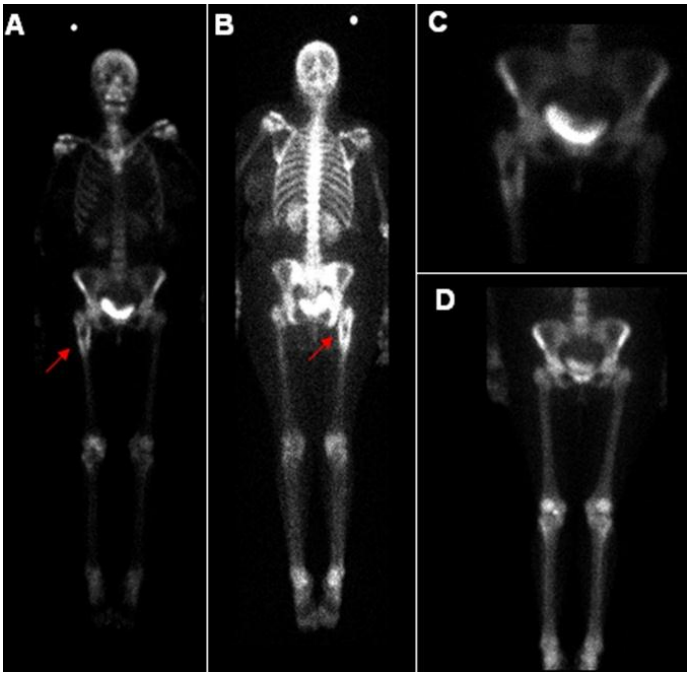

Figure 6 (right): 43 year old female with malignant phyllodes tumor. Bone scan utilizing 25.5 mCi Tc99m labeled MDP with acquisition of delayed planar and spot images.
6A: Anterior total body: Increased radiotracer uptake in the proximal right femur (red arrow).
6B: Posterior total body: Increased radiotracer uptake in the proximal right femur (red arrow).
6C: Anterior spot view of the pelvis: Increased radiotracer uptake in the proximal right femur (red arrow).
6D: Anterior total body (8 months prior to figures 6A-6C): No increased radiotracer uptake.

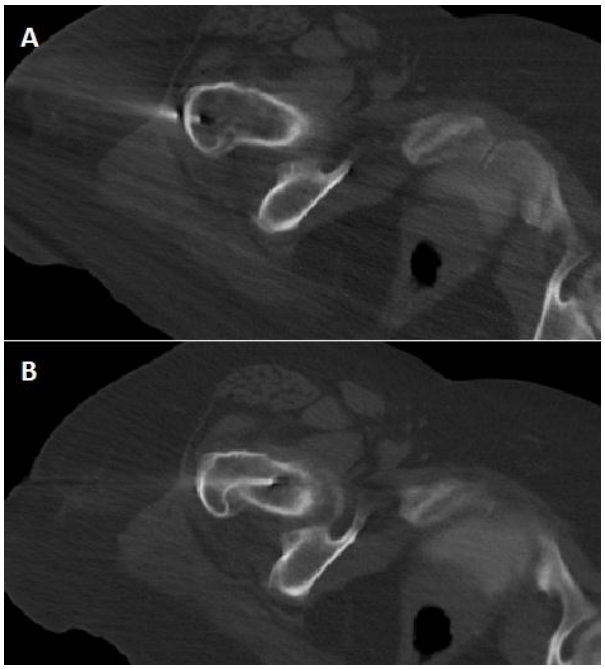

Figure 7 (left): 43 year old female with malignant phyllodes tumor. CT guided bone biopsy. Coaxial system of bone needles advanced under CT guidance into the intertrochanteric region where the permeative pattern was best visualized.
7A: Axial CT (bone window, ww/wl 2000/600): First needle pierces the lateral femoral cortex.
7B: Axial CT (bone window): Now in position, a biopsy is taken.

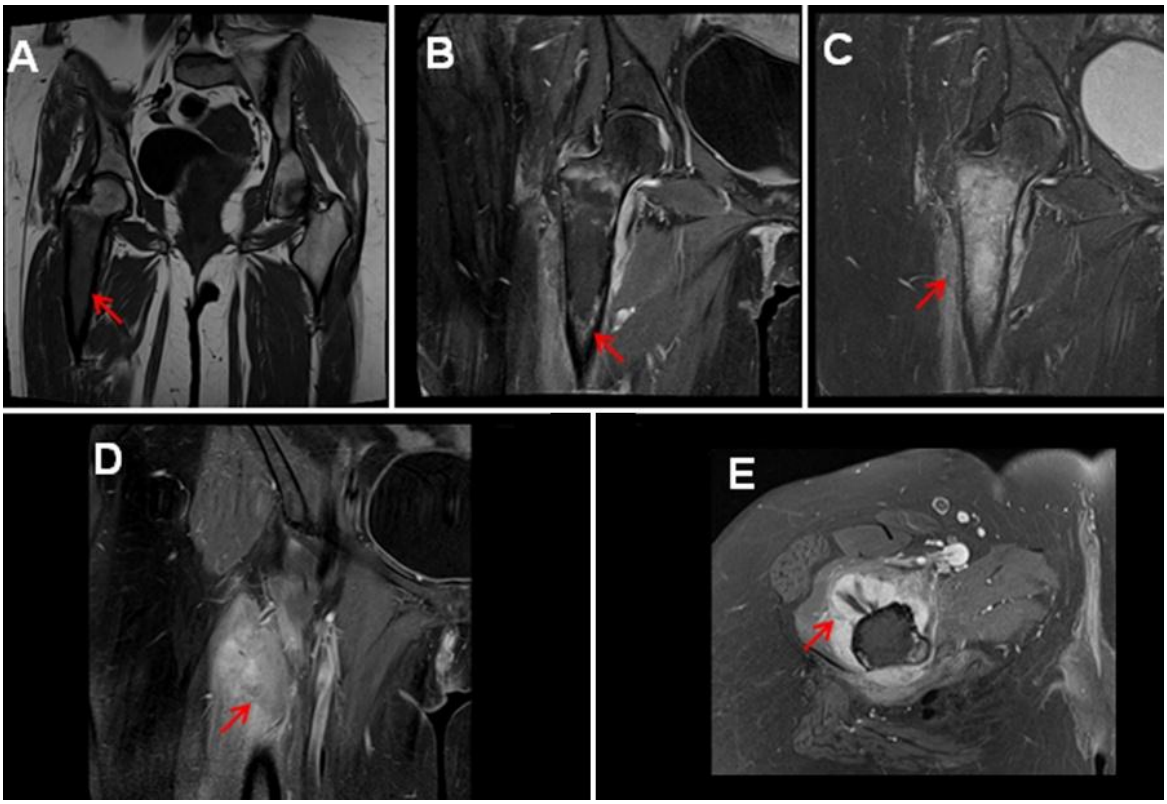

Figure 8: 43 year old female with malignant phyllodes tumor. Contrast enhanced MRI of the right femur (Siemens Avanto 1.5 tesla)
8A: Non-enhanced non-fat suppressed coronal T1 weighted image (T1W) (TE 11 / TR 641): Abnormal low signal intensity is present beginning at the intertrochanteric region and extending through the medullary cavity of the femur (red arrow).
8B: Contrast enhanced fat suppressed (17 ml gadobenate dimeglumine) coronal T1W image (TE 8.9 / TR 673): Abnormal enhancement along the periphery (red arrow) of the area of low signal intensity seen in 8A. There is also enhancement in the surrounding soft tissues.
8C: Non-enhanced coronal short tau inversion recovery image (TE 41 / TR 3000): Increased signal intensity throughout the area of abnormal signal seen on 8A and extending into the surrounding soft tissue (red arrow).
8D: Contrast enhanced (17 ml gadobenate dimeglumine) fat suppressed coronal T1W image (TE 8.9 / TR 673): Anterior to 8C, there is an enhancing soft tissue mass (red arrow) superficial to the femoral cortex.
8E: Contrast enhanced (17 ml gadobenate dimeglumine) fat suppressed axial T1W image (TE 8.9 / TR 640): Corresponding to the same mass in 8D, there is an enhancing soft tissue mass superficial to the femoral cortex (red arrow).

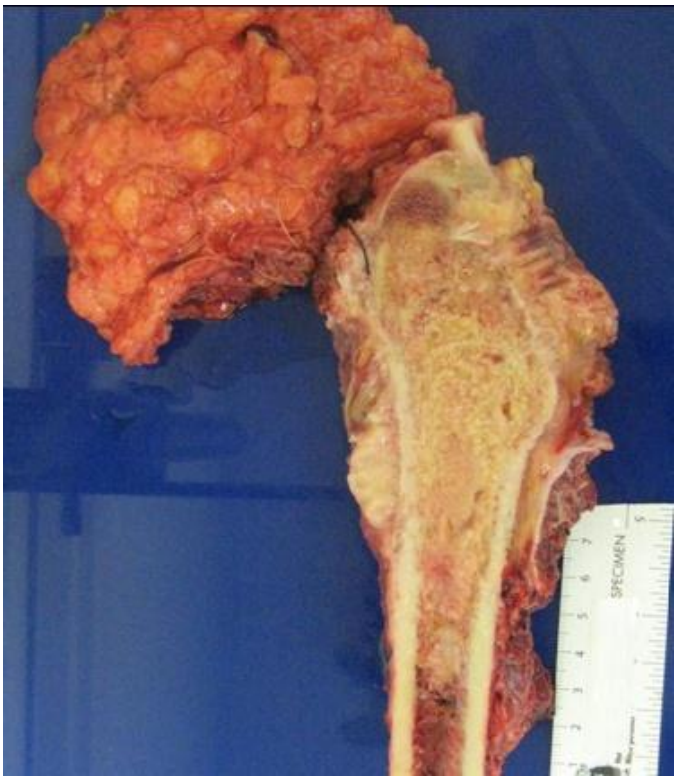

Figure 9: 43 year old female with malignant phyllodes tumor. Gross surgical specimen following resection with demonstration of medullary cavity tumor infiltration, cortical destruction and tumor adherent to the external cortical surface.

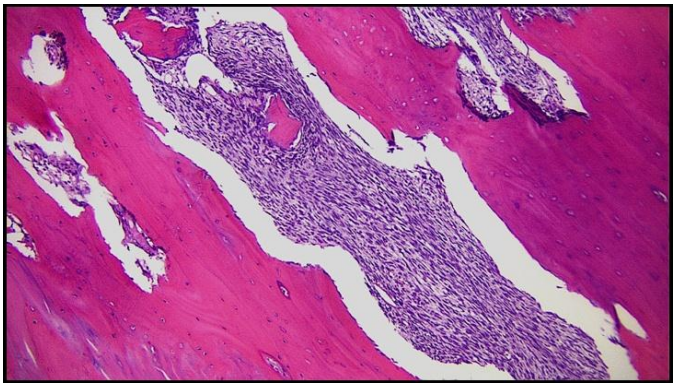

Figure 10: 43 year old female with malignant phyllodes tumor. Metastatic phyllodes tumor infiltration of the right femoral medullary cavity. H&E section, 10x magnification.

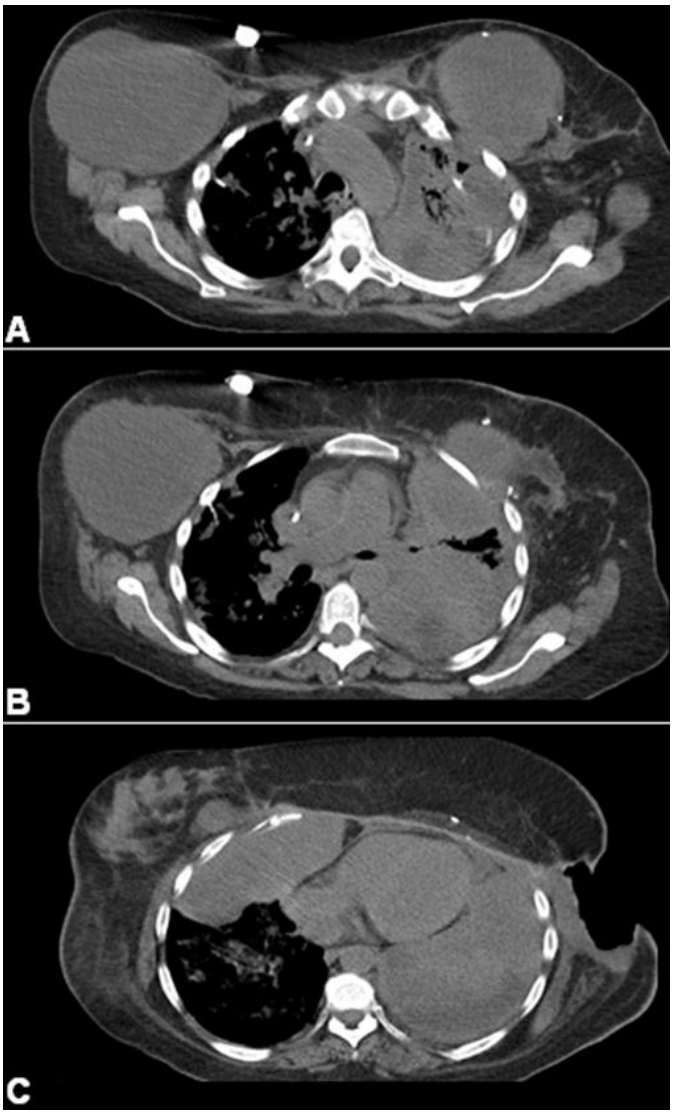

Figure 11: 43 year old female with malignant phyllodes tumor. Non-enhanced chest CT. 305 mAs, 120 kVP, 1.5 mm slices.
11A-C (abdominal window): Large soft tissue masses are present in the left chest and right axilla. There is extensive bilateral pleural disease. Lung windows (not shown) demonstrate significant pulmonary parenchymal involvement. Even with abdominal window settings, in the right lung, parenchymal disease can be visualized.

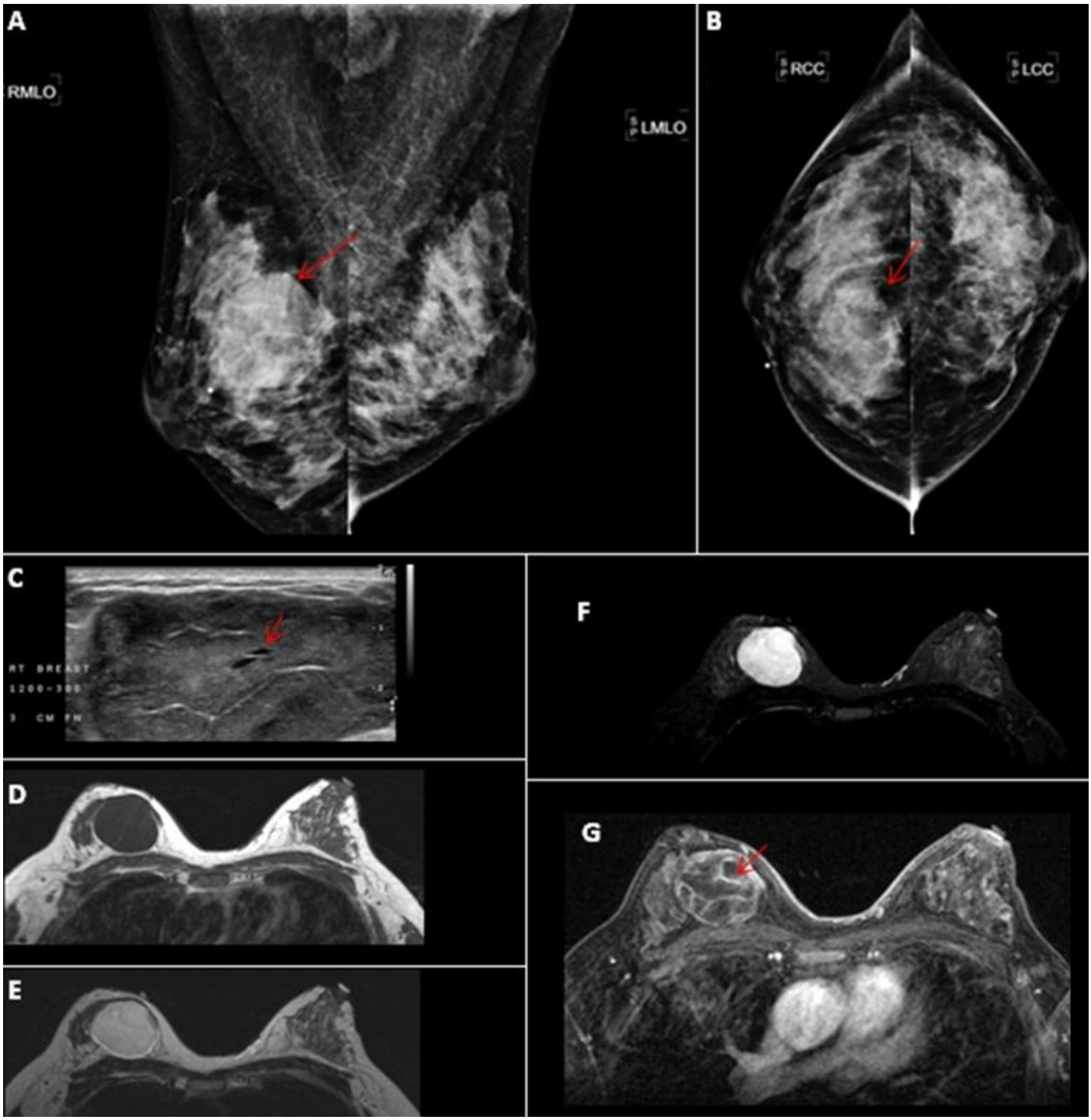

Figure 12: Pathology proven (images not shown) benign phyllodes tumor in a 42 year old female.
12A and B: Mediolateral oblique (A) and craniocaudal (B) digital diagnostic mammographic views demonstrate a large hyperdense mass in the posterior upper inner quadrant of the right breast (red arrows) without associated suspicious microcalcifications.
12C: Breast ultrasound (14 MHz linear probe) demonstrates a large heterogeneous mass at the 12-3 o'clock position 3 cm from the nipple. Within the mass, there are thin cystic clefts (red arrow).
12D: T1W (TE 12 / TR 426) non-enhanced non-fat suppressed MR image (1.5 tesla) shows a large circumscribed hypointense mass in the area corresponding to the mammographic abnormality.
12E: T2W (TE 93 / TR 3380) non-enhanced non-fat suppressed MR image (1.5 tesla) shows a large circumscribed hyperintense mass in the area corresponding to the mammographic abnormality.
12F: T2W (TE 70 / TR 5130) non-enhanced fat suppressed MR image (1.5 tesla) demonstrates a large circumscribed hyperintense mass in the area corresponding to the mammographic abnormality.
12G: 3 dimensional contrast enhanced (15 ml gadopentetate dimeglumine) fat suppressed (TE 1.43 / TR 6.44) MR image (1.5 tesla) shows enhancing septations (red arrow) and an enhancing wall associated with the mass.

Etiology:	Unknown.
Incidence:	Less than 1% of all primary breast cancers.
Gender Ratio:	Overwhelmingly female. In one study of 172 patients, all were female. There are sparse case reports of men afflicted with a phyllodes tumor [6,7].
Age Predilection:	Most commonly 35-60 years old with a median age of 45 [4,5].
Risk Factors:	Previous chest radiation therapy [4], increased prevalence in Latin white females and those of Asian descent [12].
Treatment:	Surgical excision is the primary means of treatment and selected cases may also receive radiation therapy. There is limited benefit from chemotherapy.
Prognosis:	Depends on histological grade and the presence of distant metastasis. One author describes a 5 years survival rate of malignant PT as 10% [3].
Imaging Findings:	**Mammography:** Large, hyperdense, rounded (possibly lobulated) mass with distinct margins and without malignant microcalcifications.
	Breast ultrasound: Large, hypoechoic solid mass which may contain macrocysts or thin cystic clefts. The shape may be oval, round or lobulated and the posterior acoustic behavior is non-specific. There is varying internal vascularity. Early reports suggest elastography demonstrates an elastic center with an inelastic periphery ("ring sign").
	CT: The primary tumor and metastases may appear as a heterogeneous enhancing mass which may contain solid and cystic components.
	MRI: Heterogeneous and either isointense or hypointense on T1 weighted images. Hemorrhage may result in increased T1 signal intensity. Hypointense on T2 weighted images, except in the presence of cystic spaces/necrosis. There are often internal septations which tend to be hypointense on T1 and T2 weighted images. These masses often enhance heterogeneously following contrast administration with suspicious kinetics present in 33% of cases. Though rare, enhancing septations have been described. There may be low ADC. There may be increased T2 signal in the tissue surrounding the tumor.
	Tc 99m MDP bone scan: Metastases will demonstrate increased Tc99m MDP radiotracer activity.
	Radiographs: Metastases to bone may result in a permeative or moth eaten appearance to the involved bone. There may be periosteal reaction and an adjacent soft tissue mass may be evident.

Table 1: Summary table for phyllodes tumor

Etiology	Mammography	Breast Ultrasound	MRI	CT	Bone Scan	Radiograph
Phyllodes tumor	Large, round hyperdense mass with distinct margins and without malignant micro-calcifications	Large, hypoechoic solid mass which may contain macrocysts or thin cystic clefts. The shape may be oval, round or lobulated and the posterior acoustic behavior is non-specific. There is varying internal vascularity. Early reports suggest elastography demonstrates an elastic center with an inelastic periphery.	T1: Heterogeneous and either isointense or hypointense. Hemorrhage may increase signal. T2: Hypointense, except in the presence of cystic spaces. There are often internal septations which tend to be hypointense on T1 and T2 weighted images. There may be increased signal in the tissue surrounding the mass. T1 + contrast: Enhance heterogeneously following contrast administration with suspicious kinetics present in 33% of cases. Rare septal enhancement. ADC: May be low.	Heterogeneous enhancing mass which may contain solid and cystic components including irregular enhancing septations.	Not applicable as this is not utilized to work up a breast mass. Metastases will demonstrate increased Tc99m MDP radiotracer activity.	Not applicable as this is not utilized to work up a breast mass. Metastases to bone may result in a permeative or moth eaten appearance. There may be periosteal reaction and/or an adjacent soft tissue mass.
Invasive ductal carcinoma	Spiculated, irregular mass; may also see architectural distortion or simply an asymmetry (focal or global).	Varies. Classically, hypoechoic solid mass with internal vascularity, irregular margins (including angulated or spiculated) and posterior acoustic shadowing. There may be microcalcifications and the orientation may be antiparallel. Some may also be associated with low elasticity.	T1: Irregular mass. T2: Hypointense unless necrosis (necrotic areas hyperintense) T1 + contrast: Mass like enhancement with irregular margins. Suspicious enhancement includes early enhancement with washout kinetics.	Dense irregular mass; typically used for staging and not for workup of a breast mass.	Not applicable as this is not utilized to work up a breast mass.	Not applicable as this is not utilized to work up a breast mass.
Ductal carcinoma in situ	Malignant microcalcifications such a fine linear branching and pleomorphic types with or without a mass.	Varies. May see microcalcifications as echogenic foci without or with posterior acoustic shadowing. There may be dilated ducts and a mass may or may not be seen. There may be increased vascularity.	T1: Often appears similar to glandular tissue (occult). T2: Often appears similar to glandular tissue (occult). T1 + contrast: non-mass like clumped enhancement with a segmental distribution.	Not used to work up ductal carcinoma in situ.	Not applicable as this is not utilized to work up a breast mass.	Not applicable as this is not utilized to work up a breast mass.
Giant fibroadenoma	Large, rounded mass with or without coarse "popcorn like" calcifications.	Oval or round, sometimes gently lobulated large homogeneous hypoechoic parallel mass. There may be large coarse calcifications with posterior acoustic shadowing (depends on the calcifications and fibrous component).	T1: Depends on cellularity. Low cellularity = isointense. T2: Depends on cellularity. Low cellularity = isointense. T1 + contrast: Depends on cellularity. May have homogeneous rapid enhancement. There may be non-enhancing internal septations.	May see a dense well circumscribed mass, but this is not typically used to work up a fibroadenoma.	Not applicable as this is not utilized to work up a breast mass.	Not applicable as this is not utilized to work up a breast mass.
Primary breast sarcoma	Depends on histology.	Depends on histology.	Depends on histology.	Depends on histology.	Not utilized to work up a breast mass.	Not utilized to work up a breast mass.

Table 2: Differential diagnosis based on imaging characteristics for phyllodes tumor

ABBREVIATIONS

phyllodes tumor = PT
cm = centimeter
mm = millimeter
CT = computed tomography
cGy = centigray
MRI = magnetic resonance imaging
MDP = methylenediphosphonic acid
Tc99m = technetium 99 metastable
ER = estrogen receptor
PR = progesterone receptor
FNA = fine needle aspiration

KEYWORDS

phyllodes; cystosarcoma phyllodes; breast cancer; mesenchyal breast tumor; metastatic; enhancing septations

ACKNOWLEDGEMENTS

Thank you to Dr. Isabelle Ray-Coquard and Philippe Cousin for sharing their data with us.